The Astrophysical Journal, 699:L59–L63, 2009 July 10 doi:10.1088/0004-637X/699/2/L59

SECONDARY RADIATION FROM THE PAMELA/ATIC EXCESS AND RELEVANCE FOR *FERMI*

E. Borriello[1], A. Cuoco[2], and G. Miele[1]
[1] Dipartimento di Scienze Fisiche, Università di Napoli "Federico II" & INFN Sezione di Napoli, Complesso Universitario di Monte S. Angelo, Via Cinthia 80126, Napoli, Italy
[2] Department of Physics and Astronomy, University of Aarhus, Ny Munkegade, Bygn. 1520 8000, Aarhus, Denmark
Received 2009 March 16; accepted 2009 May 14; published 2009 June 17

ABSTRACT

The excess of electrons/positrons observed by the Pamela and ATIC experiments gives rise to a noticeable amount of synchrotron and inverse Compton scattering (ICS) radiation when the e^+e^- interact with the Galactic magnetic field, and the interstellar radiation field (ISRF). In particular, the ICS signal produced within the weakly interacting, massive particle annihilation interpretation of the Pamela/ATIC excess shows already some tension with the EGRET data. On the other hand, one year of *Fermi* data taking will be enough to rule out or confirm this scenario with a high confidence level. The ICS radiation produces a peculiar and clean "ICS Haze" feature, as well, which can be used to discriminate between the astrophysical and dark matter (DM) scenarios. This ICS signature is very prominent even several degrees away from the galactic center, and it is thus a very robust prediction with respect to the choice of the DM profile and the uncertainties in the ISRF.

Key words: cosmic rays – dark matter – Galaxy: general – gamma rays: observations – ISM: general – radio continuum: ISM

The Pamela and ATIC results have recently raised great interest in the scientific community due to the possibility that the observed e^+e^- excesses could be a signature of the, so-far elusive, particle associated with dark matter (DM). The rise in the positron fraction above 10 GeV until ∼100 GeV seen by Pamela (Adriani et al. 2009a) and the excess of the sum of e^+ and e^- between ∼100 GeV and ∼700 GeV seen by ATIC (Chang et al. 2008) hardly can be explained in a standard cosmic-ray production scenario and, instead, seem to point to a new source of e^+ and e^-. Hints of this anomaly were reported also by different experiments such as HEAT (Barwick et al. 1997), AMS-01 (Aguilar et al. 2007; Alcaraz et al. 2000), and PPB-BETS (Torii et al. 2008). In addition, H.E.S.S. has recently presented a measurement of the electron spectrum in the range $0.6 < E < 5$ TeV (Aharonian et al. 2008). This anomaly can have a standard astrophysical interpretation (Atoian et al. 1995; Hooper et al. 2009; Profumo 2008), or an exotic one involving decaying (Liu et al. 2008, Hisano et al. 2008; Yin et al. 2009) or the annihilation of DM particles (Hisano et al. 2008; Arkani-Hamed et al. 2009, Cholis et al. 2008b, Bergstrom et al. 2008b; Mardon et al. 2009; Meade et al. 2009). The latter description, in particular, seems to favor a DM particle in the TeV range and with a thermally averaged annihilation cross section $\langle\sigma_A v\rangle \sim 10^{-23}$ cm^3 s^{-1}. However, this scenario faces several difficulties. A first problem is that, differently from the positron ratio, no excess is observed by Pamela in the antiproton over proton ratio (Adriani et al. 2009b). This means that DM decay/annihilation into hadronic channels is mainly forbidden or at least strongly suppressed (Cirelli et al. 2009; Donato et al. 2009), and hence one has to resort to models in which only the leptonic channels are allowed. The second problem is that the annihilation rate required to explain the anomaly is about 3 orders of magnitude above the natural expectation of $\langle\sigma_A v\rangle \sim 3 \times 10^{-26}$ cm^3 s^{-1} for a DM thermal relic which accounts for the cosmological DM abundance. This requires either the introduction of large annihilation boost factors from the presence of galactic substructure, or some enhancing annihilation mechanism such as the Sommerfeld process (Lattanzi & Silk 2008).

The fact that hadronic channels have to be suppressed to explain the Pamela/ATIC anomaly implies that only few (energetic) photons are produced either if the annihilation takes place through the $\mu^+\mu^-$ or $\tau^+\tau^-$ channels or in the case of the e^+e^- channel through the presence of final state radiation. With the limited contribution of gamma rays accompanying the annihilation process, the constraints from gamma observations become thus quite weak. Anyway, even though only e^+e^- were produced in the DM annihilation process, these leptons, once in the galactic environment, would interact with the Galactic magnetic field (GMF) and the interstellar radiation field (ISRF). Thus, they would lose energy producing synchrotron radiation in the radio band and inverse Compton scattering (ICS) radiation in the gamma band. This secondary radiation thus represents a complementary observable to constrain the DM signal (Zhang et al. 2008, Cholis et al. 2008a; Nardi et al. 2009; Ishiwata et al. 2009, Bergstrom et al. 2008a; Bertone et al. 2009; Borriello et al. 2009). In the following, we will focus on the synchrotron and ICS signals which are expected in the galactic halo. With respect to focusing on the Galactic center (GC), this approach provides much more robust predictions due to the weaker dependence on the choice of the DM profile and thanks to the smaller uncertainties on ISRF and GMF. The relevance of ICS signal in relation to Pamela has been, indeed, discussed in recent papers(Zhang et al. 2008, Cholis et al. 2008a) which show the presence of some tension with the EGRET data as well. In the following, we will stress how the situation is expected to change with the new data from *Fermi* and, further, we will investigate the peculiar spatial distribution which the DM signal is expected to produce.

We use for the calculations a slightly modified version of Galprop v50.1p (Strong & Moskalenko 1998; Moskalenko & Strong 1998), which solves numerically the electron diffusion-loss equation and produces the ICS and synchrotron maps. The code also provides maps of the cosmic ray (CR) gamma diffuse emission using available data on the CR abundances and the distribution of galactic gas. For our calculations, we employ a diffusion coefficient $D = D_0(E/E_0)^{-\alpha}$ with $D_0 = 5 \times 10^{28}$ cm^2 s^{-1}, $E_0 = 3$ GeV, and $\alpha = 0.33$, corresponding to

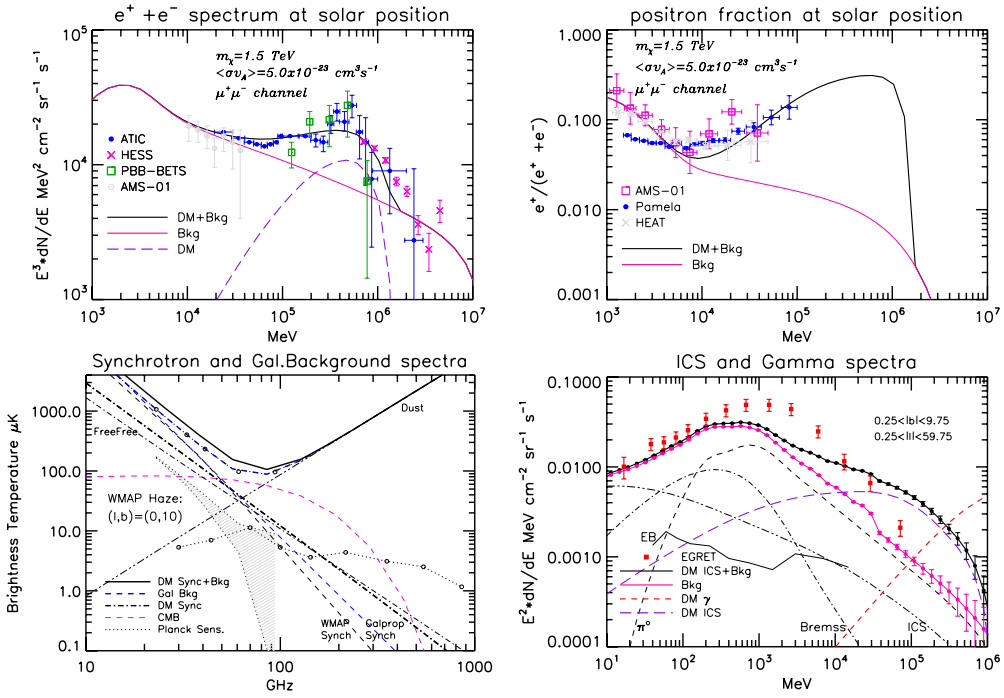

Figure 1. Upper panels show the positron fraction and the total e^+e^- spectrum for the CR background and the DM annihilation signal compared with the Pamela and ATIC data. A compilation of previous data (HEAT; Barwick et al. 1997) and AMS-01 (Aguilar et al. 2007) for the positron fraction and PPB-BETS (Torii et al. 2008), AMS-01 (Alcaraz et al. 2000), and H.E.S.S. (Aharonian et al. 2008) for the e^+e^- spectrum) is also shown. The lower right panel reports the gamma spectrum for the CR background and the ICS signal from DM electrons in the halo together with the EGRET measurements and the errors expected after a one year survey by *Fermi*. The red dashed curve shows the spectrum of gamma rays produced directly through the annihilation into $\mu^+\mu^-$. The decomposition of the CR background into the IC, bremsstrahlung, pion decay, and extragalactic components is reported as well. The lower left panel shows the DM synchrotron emission, in units of brightness temperature, 10° away from the GC compared with the galactic backgrounds as measured by *WMAP* (Gold et al. 2009) and the rms fluctuations of the CMB. The open points indicate the nine Planck frequencies, while the dotted line shows the expected Planck sensitivity for a 14 months survey (Planck Collaboration 2006). The second set of open points indicates the *WMAP* frequencies. For comparison, it is shown the signal from the *WMAP* Haze 10° away from the GC as derived in Dobler & Finkbeiner (2008). Furthermore, we report the decomposition of the Galactic backgrounds into the dust, free–free, and synchrotron components together with the synchrotron background derived with Galprop. A model with a WIMP of $m_\chi = 1.5$ TeV which annihilates only into $\mu^+\mu^-$ with a rate $\langle\sigma_A v\rangle \sim 5 \times 10^{-23}$ cm^3 s^{-1} is considered for all the plots. The propagation parameters are specified in the text.

a Kolmogorov spectrum of turbulence. The transport equation is solved in a cylinder of half-height $z = \pm 4$ kpc and radius $R = 20$ kpc, while the GMF used to derive the synchrotron radiation is modeled as $< B^2 >^{1/2} = B_0 \exp(-r/r_B - |z|/z_B)$ with $B_0 = 11\mu$G, $r_B = 10$ kpc, and $z_B = 2$ kpc. It is worth reminding, however, that electrons have typically a quite short propagation length (in terms of the galactic size) corresponding to a path of $\mathcal{O}(1$ kpc) (Delahaye et al. 2008) before losing a significant percentage of their energy. Thus, the final spectrum and distribution of electrons keep only a weak dependence on the chosen propagation parameters. The GMF, on the other hand, is still affected by large uncertainties especially in the inner kpc's of the galaxy (see Han 2009 and references therein for a recent review). The synchrotron radiation, which is quite dependent on the GMF, shares, thus, a similar uncertainty on the normalization. The ISRF, which is the photon target that determines the ICS signal, is, instead, better known and the derived ICS signal is thus a more robust prediction than the synchrotron signal. The ISRF implemented in Galprop is described in detail in Porter & Strong (2005). Finally, for the DM profile, we choose a very conservative isothermal cored one, namely $\rho(r) = \rho_0(r_c^2 + r_\odot^2)/(r_c^2 + r^2)$, with a DM density $\rho_0 = 0.4$ GeV cm^{-3} at the solar position $r_\odot = 8.5$ kpc. We fix $r_c = 2.8$ kpc for the core size. However, this particular choice is not crucial since we are going to calculate the signal not in GC, but the one coming from the halo where the uncertainties on the details of DM profile are less relevant.

We choose to study a single benchmark model with a weakly interacting, massive particle (WIMP) of $m_\chi = 1.5$ TeV annihilating in the $\mu^+\mu^-$ channel only with a rate $\langle\sigma_A v\rangle \sim 5 \times 10^{-23}$ cm^3 s^{-1}. The resulting electron/positron injection spectrum dN_e/dE has approximately a constant behavior in energy with a cutoff at the mass of the WIMP. We calculate dN_e/dE with DarkSUSY (Gondolo et al. 2004), which, in turn, uses a tabulation of the spectrum of the decay products derived with Pythia (Sjostrand et al. 2008). The electron source term for Galprop is then given by $Q(r, E) = \rho^2 \langle\sigma_A v\rangle / 2m_\chi^2 \times dN_e/dE$. This model provides a reasonable good match with the Pamela and ATIC data. It is certainly possible to achieve a better fit with a mixing of the various leptonic channels, or with a particular alternative annihilation mechanism or, further, with a fine tuning of the propagation parameters.[3] However, since the aim of our Letter is to focus on the secondary radiation, the final results would be only weakly affected by the above details on the WIMPs annihilation process. The results are illustrated in Figure 1. The upper panels show the comparison of the model with the Pamela and ATIC data

[3] During the review procedure of our Letter, the Fermi collaboration has reported a measurement of the e^+e^- flux in the same energy range of ATIC (Abdo et al. 2009). The spectrum measured by *Fermi* confirms an excess with respect to the conventional cosmic ray model although the excess is less prominent and smoother than the one reported by ATIC. For this broad smooth excess a better fit can be achieved through an annihilation into $\tau^+\tau^-$ instead of $\mu^+\mu^-$. Using the $\tau^+\tau^-$ channel as benchmark model, however, produces just minor changes in the results derived in the following.

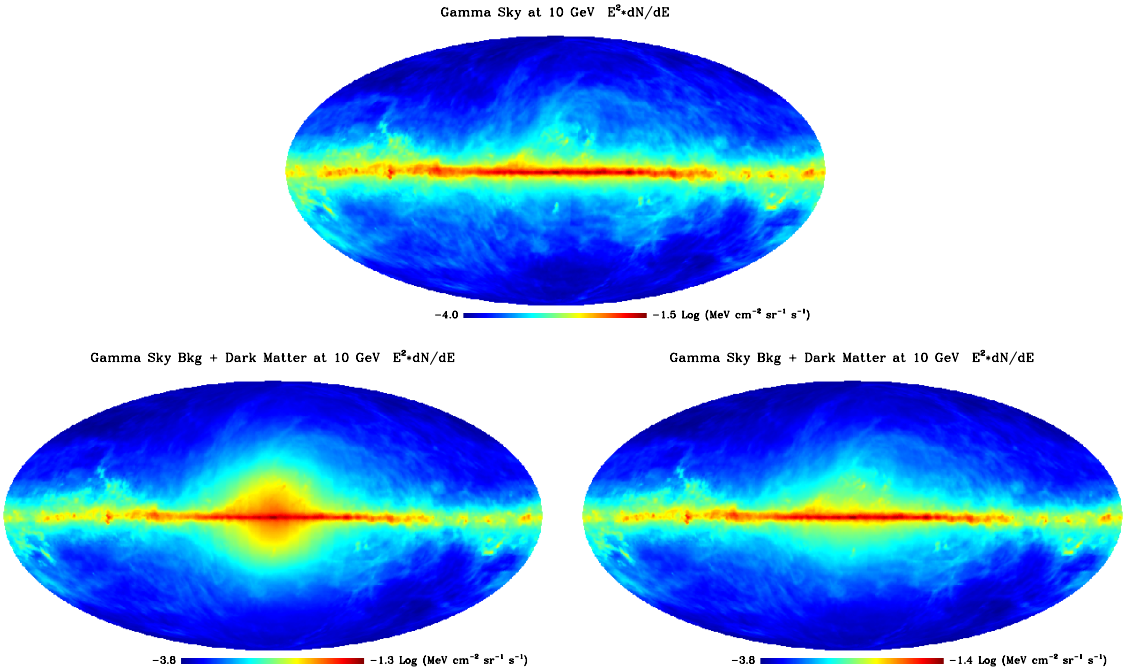

Figure 2. Sky map (in healpix format; Gorski et al. 2005) of galactic gamma backgrounds at the energy of 10 GeV (top). The same with the inclusion of the DM annihilation contribution (bottom left) or decaying DM (bottom right).

and with a compilation of previous data showing that, indeed, the agreement is good. The secondary radiation results are shown in the lower panels. The right one shows the expected difference between the CR gamma background and the ICS produced by the population of DM electrons distributed in the galactic halo together with the EGRET measurements (as taken from Strong et al. 2004b). Furthermore, the decomposition of the CR background into the IC, bremsstrahlung, pion decay, and extragalactic components is also shown. The extragalactic component (Sreekumar et al. 1998) is from the re-analysis of the EGRET data from Strong et al. (2004a). The small error bars are a forecast for $T = 1$ year of data taking by *Fermi* assuming the effective area as a function of energy as taken from Atwood et al. (2009) (roughly $A_{\rm eff} = 8000\,{\rm cm}^2$ above $\sim$1 GeV) a field of view of 2.4 sr and no CR contamination, hence $N_\gamma = T \times {\rm fov} \times f_\Delta \times \int_{\Delta E} A_{\rm eff}(E) dN_\gamma/dE(E) dE . dN_\gamma/dE(E)$ is the gamma-ray flux, while f_Δ is the fraction of area of the sky where the signal is integrated. The Poisson error is then $\propto 1/\sqrt{N_\gamma}$. Finally, the errors are shown for a logarithmic binning of the energy.

It is worth noting that the errors expected for one year from *Fermi* survey are tiny enough to detect the excess with a high degree of confidence. Even more importantly, this excess comes from the halo region, placed several degrees away from the GC and thus in a region where the uncertainties on the DM profile are expected to be much smaller. Also the uncertainty on the ISRF, which seems anyway not critical (Porter & Strong 2005), naturally decreases moving away from the GC. A possible problem is, in principle, the fact that the DM excess can be mistaken with a not well-understood CR gamma background. Indeed, the situation is similar to the EGRET GeV excess (Hunter et al. 1997) which, in principle, can be explained either with an "optimized" CR model (Strong et al. 2004b) or with a DM contribution (deBoer et al. 2005).[4] In this case, however, the IC excess produced by Pamela/ATIC is more properly a "10–100 GeV excess." Moreover, it generally exceeds already the EGRET data, although by an amount which is still in principle within the EGRET systematics. A more crucial difference is however the spatial distribution. While the GeV excess is almost isotropic in the sky, the ICS excess has the shape of a circular Haze reflecting the DM distribution in the halo. This difference, indeed, is quite striking, as can be seen clearly in Figure 2. The CR background instead is expected to lie mostly along the galactic plane where the astrophysical sources are located.

The lower left panel shows the DM synchrotron emission in units of brightness temperature ($T \propto \nu^{-2} F_\nu$) 10° away from the GC compared with the galactic backgrounds. We use the *WMAP* background maps (CMB subtracted) and their decomposition into synchrotron, free–free, and dust (Gold et al. 2009).[5] For illustration, the frequency spectra in the plot are extrapolated also outside the *WMAP* frequency coverage. We also show for comparison the background synchrotron emission calculated with Galprop which, indeed, exhibits a close match with the *WMAP* synchrotron spectrum in the 20–100 GHz range. It has to be noted that the synchrotron galactic CR emission dominates the background only up to a frequency of $\sim$60 GHz, then there is a small frequency window which is dominated by free–free (thermal bremsstrahlung) emission, while above $\sim$100 GHz the background is dominated by dust emission. The fluctuations of the CMB dominates around $\sim$100 GHz depending on the galactic latitude. The high-quality data from *WMAP*, however, allow us to efficiently clean this further "background." The DM synchrotron radiation would exhibit in principle a peak with respect to the synchrotron background around a frequency $\sim 10^5$ GHz (as shown in Zhang et al. 2008), where, however, the dust background is dominating by many orders of magnitude. Restricting the analysis in the more interesting frequency range $<$1000 GHz, the DM signal has an almost power-law behavior with a slope slightly harder than the background, while the

[4] Note, anyway, that preliminary results from the Fermi collaboration seem not to confirm the GeV excess. See, e.g., the talk presented on behalf of the Fermi collaboration at the 2009 January meeting of the AAS.

[5] Data are available at the Lambda Web site: http://lambda.gsfc.nasa.gov/.

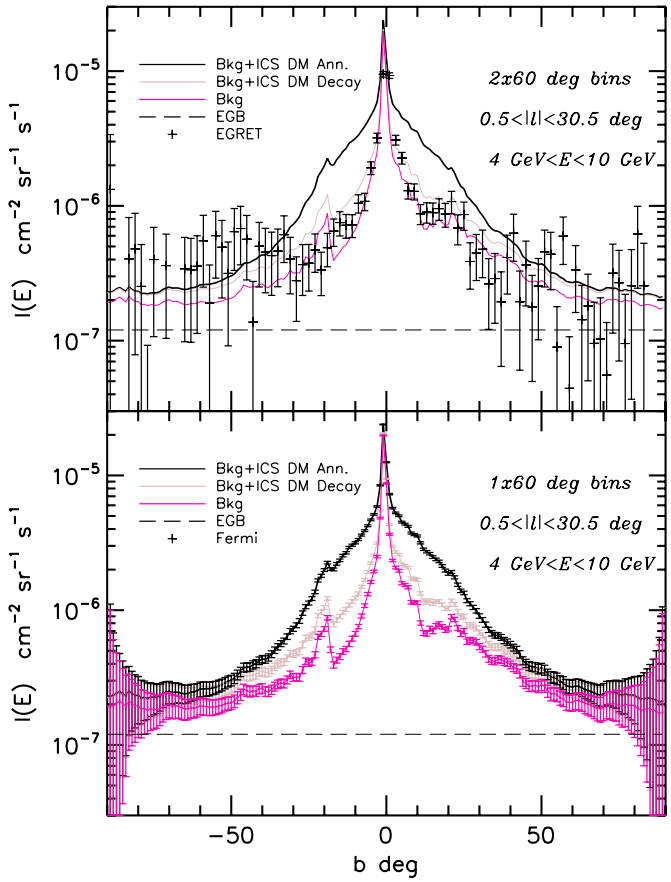

Figure 3. Top panel: background and DM (either annihilating and decaying) latitude gamma profiles averaged in a strip of 60° along $l = 0$ compared with the EGRET data. Bottom panel: same as above, but with the errors expected with a one year survey from Fermi. At high latitudes the error bars appear artificially to increase for the geometry of the $0.^{\circ}5 < |l| < 30.^{\circ}5$ strip (which is effectively shrinking along b).

spatial distribution has a circular shape. These characteristics indeed correspond to what is found in the *WMAP* Haze (Dobler & Finkbeiner 2007; Hooper et al. 2007) whose signal we also report in the plot for comparison. Note, however, that the Haze feature has still to be firmly established and that at the moment it is very much dependent on the method employed to separate the foregrounds (Gold et al. 2009). Interestingly, we find that, for the GMF model employed, the DM signal exceeds the Haze for a factor of ∼3 similarly to the IC case. The theoretical signal, on the other hand, is affected by the uncertainties on the GMF and it is difficult to normalize reliably. Moreover, further uncertainties come from the systematics involved in the separations of the measured signal into the various components, synchrotron, dust, free–free, and DM, hence it would be difficult to asses the real significance of this excess.

We also consider the case of electrons arising from WIMP decay considering a DM signal following linearly the halo profile and with the same electron injection spectrum as for the $\mu^+\mu^-$ channel. Formally, at the solar position, up to diffusion effects, exactly the same positron fraction and electron spectrum can be obtained setting the DM decay rate to $\Gamma = \rho_0 \langle \sigma_A v \rangle / 2 m_\chi$. The ICS radiation from the halo is however significantly reduced although Fermi can still discriminate this possibility as shown in Figures 2 and 3. At this level, however, the confusion with a not well understood background could become more problematic although the peculiar circular shape of the ICS Haze, present also in this case (see Figure 2), can help to distinguish the DM signal from the astrophysical background.

Finally, in Figure 3, we report another forecast example of the excellent *Fermi* ability to discriminate among the astrophysical and annihilating DM scenario considering the latitude profile and a strip of 60° width along $l = 0$. We also show in the upper panel the EGRET data in the same region and energy range (as derived with the Galplot package; see also Strong et al. 2004b). Compared with the EGRET data the annihilation model seems to produce a too much broad peak to fit the data, beside producing an excessively high normalization. The decaying model is instead difficult to separate from the background within the EGRET error bars. With the upcoming *Fermi* data at hands, the analysis easily can be generalized to exploit the full angular shape of the IC Haze. This would clearly offer the optimal sensitivity to disentangle the different scenarios.

In summary, we have shown that *Fermi* has the potential to test the DM interpretation of Pamela/ATIC basically in a model-independent way, thanks to the strong IC signal which the Pamela/ATIC electrons would themselves produce in the galactic halo. The EGRET data seem, indeed, already to disfavor the DM annihilation interpretation. Further, the IC signal gives rise to a striking "IC Haze" feature peaking around 10–100 GeV which would provide a further mean to discriminate the DM signal from the astrophysical backgrounds and/or to check for possible systematics.

G. Miele acknowledges support from INFN–I.S. FA51 and PRIN 2006 "Fisica Astroparticellare: Neutrini ed Universo Primordiale" of Italian MIUR.

REFERENCES

Abdo, A., et al. (Fermi Collaboration) 2009, Phys. Rev. Lett., 102, 181101
Adriani, O., et al. (PAMELA Collaboration) 2009a, Nature, 458, 607
Adriani, O., et al. 2009b, Phys. Rev. Lett., 102, 051101
Aguilar, M., et al. (AMS-01 Collaboration) 2007, Phys. Lett. B, 646, 145
Aharonian, F., et al. (HESS Collaboration) 2008, Phys. Rev. Lett., 101, 261104
Alcaraz, J., et al. (AMS Collaboration) 2000, Phys. Lett. B, 484, 10, (495, 440, erratum)
Arkani-Hamed, N., Finkbeiner, D. P., Slatyer, T., & Weiner, N. 2009, Phys. Rev. D, 79, 015014
Atoian, A. M., Aharonian, F. A., & Volk, H. G. 1995, Phys. Rev. D, 52, 3265
Atwood, F. W. B., et al. (LAT Collaboration) 2009, ApJ, 697, 1071
Barwick, S. W., et al. (HEAT Collaboration) 1997, ApJ, 482, L191
Bergstrom, L., Bertone, G., Bringmann, T., Edsjo, J., & Taoso, M. 2008a
Bergstrom, L., Bringmann, T., & Edsjo, J. 2008b, Phys. Rev. D, 78, 103520
Bertone, G., Cirelli, M., Strumia, A., & Taoso, M. 2009, J. Cosmol. Astropart. Phys., JCAP03(2009)009
Borriello, E., Cuoco, A., & Miele, G. 2009, Phys. Rev. D, 79, 023518
Chang, J., et al. 2008, Nature, 456, 362
Cholis, I., Dobler, G., Finkbeiner, D. P., Goodenough, L., & Weiner, N. 2008a, arXiv:0809.1683
Cholis, I., Goodenough, L., Hooper, D., Simet, M., & Weiner, N. 2008b, arXiv:0809.1683
Cirelli, M., Kadastik, M., Raidal, M., & Strumia, A. 2009, Nucl. Phys. B, 813, 1
deBoer, W., Sander, C., Zhukov, V., Gladyshev, A. V., & Kazakov, D. I. 2005, A&A, 444, 51
Delahaye, T., Lineros, R., Donato, F., Fornengo, N., & Salati, P. 2008, Phys. Rev. D, 77, 063527
Dobler, G., & Finkbeiner, D. P. 2007, 2008, ApJ, 680, 1222
Donato, F., Maurin, D., Brun, P., Delahaye, T., & Salati, P. 2009, Phys. Rev. Lett., 102, 071301
Gold, B., et al. (WMAP Collaboration) 2009, ApJS, 180, 265
Gondolo, P., Edsjo, J., Ullio, P., Bergstrom, L., Schelke, M., & Baltz, E. A. 2004, J. Cosmol. Astropart. Phys. JCAP07(2004)008

Gorski, K. M., et al. 2005, ApJ, 622, 759
Han, J. L. 2009, arXiv:0901.1165
Hisano, J., Kawasaki, M., Kohri, K., & Nakayama, K. 2008, arXiv:0812.0219
Hisano, J., Kawasaki, M., Kohri, K., & Nakayama, K. 2009, Phys. Rev. D, 79, 063514
Hooper, D., Blasi, P., & Serpico, P. D. 2009, J. Cosmol. Astropart. Phys., JCAP01(2009)025
Hooper, D., Finkbeiner, D. P., & Doblerm, G. 2007, Phys. Rev. D, 76, 083012
Hunter, S. D., et al. 1997, ApJ, 481, 205
Ishiwata, K., Matsumoto, S., & Moroi, T. 2009, Phys. Rev D, 79, 043527
Lattanzi, M., & Silk, J. I. 2008, arXiv:0812.0360
Liu, J., Yin, P. f., & Zhu, S. h. 2008, arXiv:0812.0964
Mardon, J., Nomura, Y., Stolarski, D., & Thaler, J. 2009, arXiv:0901.2926
Meade, P., Papucci, M., & Volansky, T. 2009, arXiv:0901.2925
Moskalenko, I. W., & Strong, A. W. 1998, ApJ, 493, 694
Nardi, E., Sannino, F., & Strumia, A. 2009, J. Cosmol. Astropart. Phys. JCAP01(2009)043
Planck Collaboration, "Planck: The Scientific Programme," 2006, arXiv:astro-ph/0604069
Porter, T. A., & Strong, A. W. 2005, arXiv:astro-ph/0507119
Profumo, S. 2008, arXiv:0812.4457
Sjostrand, T., Mrenna, S., & Skands, P. 2008, Comput. Phys. Commun., 178, 852
Sreekumar, P., et al. (EGRET Collaboration) 1998, ApJ, 494, 523
Strong, A. W., & Moskalenko, I. W. 1998, ApJ, 509, 212
Strong, A. W., Moskalenko, I. W., & Reimer, O. 2004a, ApJ, 613, 956
Strong, A. W., Moskalenko, I. W., & Reimer, O. 2004b, ApJ, 613, 962
Torii, S., et al. (PPB-BETS Collaboration) 2008, arXiv:0809.0760
Yin, P. f., Yuan, Q., Liu, J., Zhang, J., Bi, X. j., & Zhu, S. h. 2009, Phys. Rev. D, 79, 023512
Zhang, J., Bi, X. j., Liu, J., Liu, S. M., Yin, P. f., Yuan, Q., & Zhu, S. h. 2008, arXiv:0812.0522